



Effects of biochar content on gas diffusion coefficient of soil with different compactness and air contents

Fu Quan Chen¹ · Neng Kai Zhao¹ · Song Feng^{1,2,3} · Hong Wei Liu^{3,4} · Yu Chuan Liu¹

Received: 22 November 2019 / Accepted: 25 March 2020 / Published online: 10 April 2020
© Springer-Verlag GmbH Germany, part of Springer Nature 2020

Abstract

Biochar has been found to be a potentially suitable amendment for landfill cover material and agricultural soil. The addition of biochar can improve the physical (e.g., adsorption capacity) and hydrological properties (e.g., water/gas permeability) of soil. However, no experimental study is available about the effect of biochar content (BC) on the gas diffusion coefficient (D_p) of soil. The present study investigated the effect of BC on D_p under different degree of compaction (DOC; 85%, 90%, and 95%) and soil air contents (SAC; 5%, 10%, and 15%). It was found that DOC and BC had negligible effects on D_p when SAC was low (~5%). In contrast, when the SAC was relatively high (~15%), soil with DOC of 85% had the largest D_p for BC ranging from 0 to 15% (w/w). Only when the SAC was large (~15%), the addition of biochar generally increased D_p .

Keywords Biochar-amended soil · Degree of compaction · Soil air content · Pore characteristics · Gas diffusion coefficient

Introduction

Biochar is a kind of porous material rich in carbon, which is produced by pyrolysis of biomass in a high temperature (e.g., 300–800 °C) and oxygen-free or low-oxygen environment (Lei and Zhang 2013; Wong et al. 2016; Adhikari et al. 2019). Biochar has been proved to be a good amendment for landfill cover material and agricultural soil in recent years (Wu et al. 2017; Su et al. 2019; Wong et al. 2016; Zhang et al. 2018; Chen et al. 2019b; Chen and Ng 2013). There are many materials for producing biochar, such as wood chips, peanut shells, crop straws, and bamboo stalks (Fang et al. 2014; Garg et al. 2019; Chen et al. 2018; Senbayram et al. 2019; Shang et al. 2013).

Adding biochar to soil can change the physical and hydrological properties of soil, such as pore characteristics (Kuncoro et al. 2014), water retention capacity (Wong et al. 2017; Lei and Zhang 2013; Liu et al. 2016), and water/air permeability (Gopal et al. 2019; Chen et al. 2015, 2019a; Garg et al. 2019). Biochar-amended soil (BAS) also has good performance in harmful gas/chemical adsorption (e.g., hydrogen sulfide; Shang et al. 2013; Xu et al. 2014; and nitrate; Iberahim et al. 2018; Tan et al. 2018), mitigation of greenhouse gas emission and reduction of nitrate leaching in agricultural soil (e.g., methane, Sun et al. 2019; and NO_3 , Sanford et al. 2019), and methane oxidation capacity enhancement in landfill covers (Reddy et al. 2014; Yargicoglu and Reddy 2017).

Responsible editor: Zhihong Xu

✉ Song Feng
sfengaa@connect.ust.hk

Fu Quan Chen
phdchen@fzu.edu.cn

Neng Kai Zhao
N180520014@fzu.edu.cn

Hong Wei Liu
hliuan@connect.ust.hk

Yu Chuan Liu
Liuyuchuan@fzu.edu.cn

¹ College of Civil Engineering, Fuzhou University, Fuzhou, China

² Department of Civil Engineering, MOE Key Laboratory of Soft Soils and Geoenvironmental Engineering, Zhejiang University, Zhejiang, China

³ Formerly Department of Civil and Environmental Engineering, Hong Kong University of Science and Technology, Hong Kong, China

⁴ College of Environment and Resource, Fuzhou University, Fuzhou, China

Gas transports through soil mainly through diffusion and advection, which are driven by gas concentration difference and gas pressure difference, respectively. Diffusion is a very important way for gas flow in soils. For example, oxygen, which is essential for methane oxidation in landfill covers and root respiration in shallow soil layers, enters the soil mainly through diffusion from the atmosphere (Feng et al. 2019; Chen et al. 2019c; Lipiec et al. 2012; Wall and Heiskanen 2009). Although the influence of biochar on gas advection in soils was investigated (Garg et al. 2019; Wong et al. 2016), little attention has been paid on gas diffusion in BAS.

It has been recognized that there are many factors affecting gas diffusion coefficient (D_p) of soil, including soil air content (SAC; $\text{mm}^3_{\text{air}} \text{mm}^{-3}_{\text{soil}}$), degree of compaction (DOC), and micro-structure of soil (e.g., pore path tortuosity, pore size). (Kuncoro et al. 2014; Moldrup et al. 2000b; Resurreccion et al. 2008b; Schjønning 1989). When SAC is lower than a certain value (e.g., $\leq 10\%$), soil pores could be almost filled by water, which impedes gas diffusion (Resurreccion et al. 2008a). Some studies reported that under the same SAC, the D_p of soil would increase with DOC due to reduced water blockage effects under extreme compaction (Hamamoto et al. 2011; Millington and Quirk 1961). However, the opposite trend was found by Kuncoro et al. (2014), who attributed the reduction of D_p with the increase of DOC to the more tortuous pore path and the more vulnerable compaction of macro-pore in soil. Evidently, the influence of DOC on gas diffusion coefficient of soil is still controversial.

In this experimental study, the effect of biochar content (BC; $\text{g}_{\text{biochar}} \text{g}^{-1}_{\text{soil}}$) on D_p of the soil was investigated under different controlled DOCs and SACs. The D_p of BAS was measured by a two-chamber diffusion apparatus. To interpret the measurements, the micro-structure characteristics of BAS were investigated by scanning electron microscopy (SEM).

Materials and methods

Properties of soil and biochar

The biochar used in this study was made from fir wood chips, which was collected from wood processing plants. The biochar was produced in an oxygen-free environment at 400–800 °C (according to manufacturer). The test soil was collected from the Hongmiaoling Waste Sanitary Landfill Site in Fuzhou City, Fujian Province, China (N 26° 10' 11", S 119° 18' 13"), and was classified as silty sand (ASTM D2487 2017).

The soil and the biochar were air-dried in room temperature of 25 °C \pm 1 °C, and then sieved by a 2-mm sieve and a 0.425-mm sieve, respectively. Subsequently, the soil and biochar were stored in sealed plastic bags. The initial gravimetric water content (GWC) of the soil and biochar were measured by continuous drying for 24 h in an oven with controlled temperature of 105 °C. The specific gravities of the soil and biochar were measured according to the ASTM D854 (2014). The particle size distributions of the soil and biochar were measured according to the ASTM D422 (2007). The liquid limit, plastic limit, and plasticity index of the soil were measured according to the ASTM D4318 (2017). BAS compaction curves were measured according to the ASTM D698 (2010) to obtain the optimum moisture content (% w/w) and the maximum dry density (g/cm^3). Some basic properties of the biochar and soil were given in Table 1.

Specimen preparation

Four different contents of the air-dried biochar (0%, 5%, 10%, and 15% by dry mass) were mixed with the air-dried soil thoroughly. Then, water was added to the mixture of soil and biochar to the target GWC, which was determined based

Table 1 Basic properties of soil and biochar

Properties	Soil	Biochar	Reference
Specific gravity (g/cm^3)	2.66	2.55	ASTM D 854 (2014)
Particle size distribution (%)			ASTM D 422 (2007)
Coarse sand (2–4.75 mm)	0	0	
Medium sand (0.425–2 mm)	53.60	0	
Fine sand (0.075–0.425 mm)	26.13	65.19	
Silt (0.002 mm–0.075 mm)	15.87	27.20	
Clay (< 0.002 mm)	4.40	7.61	
Atterberg's limits			ASTM D 4318 (2017)
Liquid limit (LL) (%)	37.80	ND	
Plastic limit (PL) (%)	28.20	ND	
Plastic index (PI)	9.60	ND	
Optimum water content (%)	17.12	ND	ASTM D 698 (2010)
Maximum dry density (g/cm^3)	1.84	ND	ASTM D 698 (2010)

ND, not determined

Fig. 1 Schematic of the two-chamber apparatus for measuring gas diffusion coefficient of biochar-amended soil

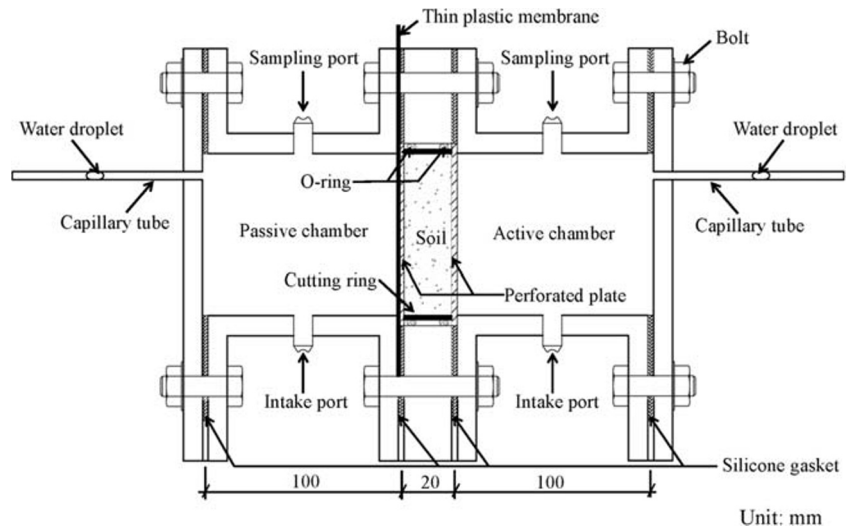


Table 2 The soil air content (SAC), gravimetric water content (GWC), degree of saturation (DS), gas diffusion coefficient (D_p), and porosity of each soil sample

Target DOC (%)	Target BC (%)	SAC (%)*	GWC (%)	DS (%)	D_p (mm ² /s)	Porosity (%)	
95	0	14.57 ± 0.286**	11.30 ± 0.293	57.51 ± 1.047	0.284 ± 0.021	34.30 ± 0.157	
		10.11 ± 0.454	13.60 ± 0.472	70.21 ± 1.578	0.164 ± 0.016	33.95 ± 0.274	
		5.27 ± 0.257	16.28 ± 0.273	84.44 ± 0.835	0.035 ± 0.007	33.84 ± 0.144	
	5	14.90 ± 0.239	11.70 ± 0.249	57.49 ± 0.859	0.359 ± 0.020	35.04 ± 0.145	
		10.10 ± 0.106	14.38 ± 0.113	71.06 ± 0.358	0.200 ± 0.061	34.91 ± 0.065	
		6.05 ± 0.279	16.26 ± 0.300	82.38 ± 0.900	0.051 ± 0.014	34.34 ± 0.169	
	10	15.55 ± 0.055	11.47 ± 0.058	55.84 ± 0.199	0.329 ± 0.008	35.22 ± 0.034	
		10.37 ± 0.168	14.58 ± 0.181	70.64 ± 0.561	0.153 ± 0.011	35.33 ± 0.102	
		5.35 ± 0.033	17.53 ± 0.036	84.87 ± 0.101	0.059 ± 0.004	35.34 ± 0.020	
	15	15.90 ± 0.135	11.59 ± 0.143	55.35 ± 0.485	0.375 ± 0.033	35.60 ± 0.077	
		10.81 ± 0.237	14.64 ± 0.257	69.71 ± 0.787	0.173 ± 0.018	35.68 ± 0.144	
		6.03 ± 0.057	17.33 ± 0.063	83.03 ± 0.177	0.067 ± 0.004	35.55 ± 0.035	
	90	0	15.45 ± 0.245	12.85 ± 0.232	58.20 ± 0.737	0.283 ± 0.040	36.96 ± 0.177
			10.02 ± 0.345	16.54 ± 0.389	74.32 ± 1.071	0.150 ± 0.001	37.48 ± 0.209
			5.86 ± 0.388	18.60 ± 0.441	84.16 ± 1.150	0.036 ± 0.011	36.97 ± 0.230
5		14.77 ± 0.184	14.59 ± 0.209	61.67 ± 0.589	0.302 ± 0.058	38.55 ± 0.128	
		11.06 ± 0.037	16.19 ± 0.042	70.72 ± 0.117	0.181 ± 0.005	37.76 ± 0.023	
		6.56 ± 0.200	18.74 ± 0.328	82.53 ± 0.640	0.075 ± 0.009	37.56 ± 0.228	
10		14.88 ± 0.123	14.96 ± 0.141	61.86 ± 0.389	0.320 ± 0.009	39.02 ± 0.075	
		10.33 ± 0.014	17.53 ± 0.017	73.34 ± 0.043	0.116 ± 0.001	38.74 ± 0.009	
		5.40 ± 0.432	19.96 ± 0.246	85.84 ± 1.032	0.053 ± 0.022	38.08 ± 0.398	
15		14.76 ± 0.076	15.64 ± 0.089	62.81 ± 0.235	0.390 ± 0.016	39.68 ± 0.046	
		10.56 ± 0.826	17.83 ± 0.974	73.03 ± 2.462	0.187 ± 0.042	39.16 ± 0.487	
		6.75 ± 0.074	19.51 ± 0.088	82.45 ± 0.213	0.044 ± 0.005	38.47 ± 0.045	
85		0	16.10 ± 0.296	15.27 ± 0.345	60.05 ± 0.911	0.454 ± 0.065	40.30 ± 0.179
			10.82 ± 0.082	18.76 ± 0.099	73.26 ± 0.237	0.238 ± 0.019	40.47 ± 0.050
			6.22 ± 0.148	21.43 ± 0.181	84.53 ± 0.401	0.054 ± 0.035	40.23 ± 0.089
	5	15.35 ± 0.129	17.09 ± 0.158	63.22 ± 0.378	0.554 ± 0.042	41.74 ± 0.078	
		10.36 ± 0.141	20.31 ± 0.176	75.16 ± 0.389	0.213 ± 0.023	41.73 ± 0.085	
		6.10 ± 0.229	22.60 ± 0.289	85.21 ± 0.605	0.058 ± 0.036	41.28 ± 0.139	
	10	16.35 ± 0.078	16.26 ± 0.095	60.60 ± 0.234	0.550 ± 0.047	41.51 ± 0.048	
		11.13 ± 0.165	19.76 ± 0.207	73.27 ± 0.461	0.248 ± 0.008	41.65 ± 0.101	
		5.99 ± 0.120	23.19 ± 0.154	85.65 ± 0.314	0.029 ± 0.020	41.73 ± 0.073	
	15	15.35 ± 0.063	18.04 ± 0.079	64.02 ± 0.181	0.549 ± 0.058	42.68 ± 0.039	
		11.05 ± 0.146	20.45 ± 0.185	73.85 ± 0.402	0.240 ± 0.053	42.25 ± 0.089	
		6.12 ± 0.208	23.64 ± 0.272	85.50 ± 0.536	0.017 ± 0.008	42.21 ± 0.127	

SAC, GWC, DS, and porosity were measured after diffusion test

**Values are presented in mean ± standard deviation

on the target DOC (85%, 90%, and 95%) and SAC (5%, 10%, and 15%). Then, the moist BAS mixture was sieved through a 2-mm sieve and was subsequently stored in sealed plastic bags for at least 24 h for moisture equilibrium. Before compaction of the soil sample, the inner wall of the sample cutting ring (internal diameter of 79.8 mm, wall thickness of 1.8 mm, and height of 20 mm) was pasted with a thin layer of Vaseline to avoid any preferential flow along the interface between the soil sample and the inner wall of the cutting ring (Allaire et al. 2008). The dry density of the mixture was determined by the measured compaction curves according to the target BC and DOC. The mixture of the soil and biochar was compacted to form a cylindrical soil sample with a diameter of 79.8 mm and a height of 20 mm. After the soil sample preparation, the test was carried out immediately to prevent the formation of a moisture gradient in the soil sample (Boon et al. 2013).

Measurement apparatus and test procedure

The D_p was measured by a two-chamber diffusion system device (Fig. 1) (Schjøning et al. 2013). The device was made of polymethyl methacrylate (PMMA). It consisted of an active chamber, a passive chamber, and a soil sample chamber in between. The inner diameter of the active chamber and passive chamber were both 80 mm, while the soil sample chamber had an inner diameter of 90 mm. All the three chambers had the same wall thickness of 10 mm. The connections between different chambers were sealed by a silicon gasket (3-mm thick). Capillary tube (internal diameter of 4 mm), sampling ports, and intake ports were installed in the active and passive chambers. Water droplets were added to the capillary tube to keep the gas pressure inside the device equal to the atmospheric pressure during the test. A soil sample contained inside the sample cutting ring was placed in the soil sample chamber. Two O-rings were installed at the gap between the outermost of the cutting ring and the inner wall of the soil sample chamber to prevent any gas preferential flow through the gap. A perforated PMMA plate (5-mm thick) with uniform distributed 4-mm diameter holes was installed at each end of the soil sample to prevent any potential soil collapse. A thin plastic membrane (0.1-mm thick) was installed between the passive chamber and soil sample chamber to block any gas exchange between the passive and active chambers through the soil before the test. The test was carried out in room with controlled temperature of $25\text{ }^\circ\text{C} \pm 1\text{ }^\circ\text{C}$.

After installing the soil sample in the device, a certain concentration of gas (O_2) was injected into the active chamber through the intake port, while pure N_2 was pumped in to the passive chamber until negligible O_2 could be measured (e.g., $< 0.1\%$) (Bonroy et al. 2011). A 5-mL air tight syringe was adopted for taking 2-mL gas samplings. The volumetric concentration of O_2 (C_0) of each gas sampling was measured by a gas

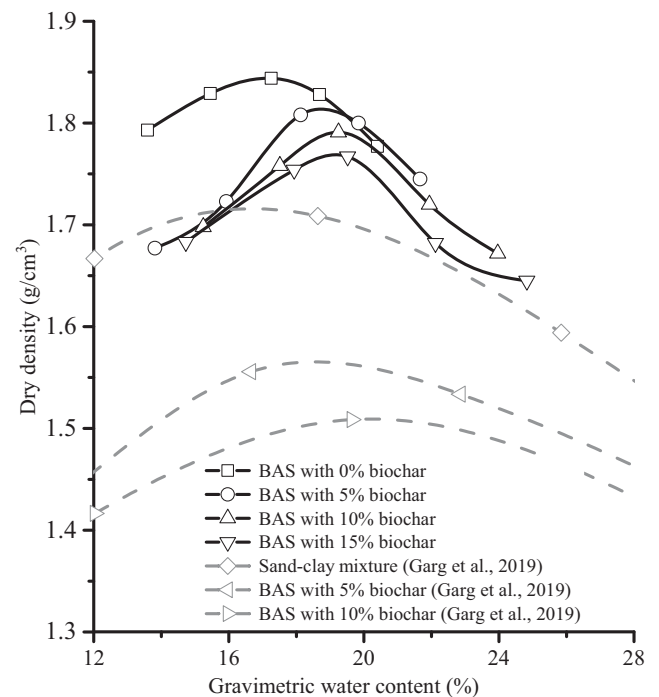


Fig. 2 Compaction curves for soils amended with different biochar contents (BCs)

chromatograph (GC112A; Shanghai INESA Scientific Instrument Co., Ltd. in Shanghai, China; measurement accuracy of 0.1% vol). The diffusion test commenced after pulling out the thin plastic membrane. The test duration was recorded by using a stopwatch. The initial gas concentration in the active chamber was measured after test begun for 15 min. This aimed to avoid (i) the potential change of gas pressure inside the device caused by the change of chamber volume at the moment of pulling out the thin plastic membrane, and (ii) the associated non-diffusive gas

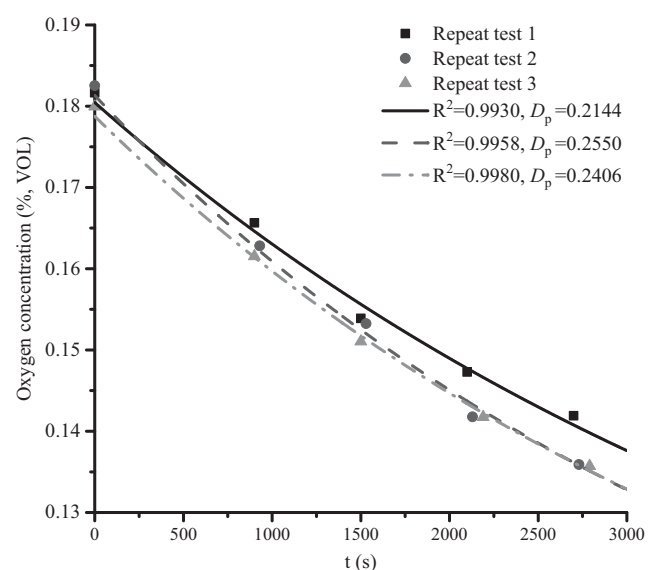


Fig. 3 The measured and fitted temporal variations of oxygen concentration in the active chamber for a set of replicated tests

flow through the soil sample (Schjønning et al. 2013). Then, a 10-min interval was adopted for the subsequent gas samplings. Five gas samplings were taken for each test.

Measurement of D_p

During the test, the device was completely sealed, and the pressure inside the device was always equal to the atmospheric pressure. Therefore, the gas diffusion in the chamber satisfied Fick’s second law (Dane and Topp 2002). The D_p in the soil sample can be calculated from the temporal variation of oxygen concentration inside the active chamber by the following formula (Glauz and Rolston 1989):

$$\ln \left\{ \frac{B(\alpha_1)}{A(\alpha_1)} \left[\frac{1}{2(1 + L\varepsilon/H)} - \frac{C_g}{C_0} \right] \right\} = -\frac{D_p \alpha_1^2}{L^2 \varepsilon} t \quad (1)$$

where D_p is the gas diffusion coefficient of BAS ($\text{mm}^3_{\text{air}} \text{mm}^{-1}_{\text{soil}} \text{s}^{-1}$), t is the diffusion time (s), ε is the soil air content ($\text{mm}^3_{\text{air}} \text{mm}^{-3}_{\text{soil}}$), L is half the height of the soil sample (10 mm), H is the height of the active/passive chamber

(100 mm), C_g is the volumetric concentration of O_2 within the active chamber at time t (mL/mL); α_1^2 is defined by the following equation when the sizes of the active and passive chambers are the same (Glauz and Rolston 1989):

$$\alpha_1^2 = \frac{1}{\beta} - \frac{1}{3\beta^2} + \frac{4}{45\beta^3} + \frac{16}{945\beta^4} + \dots \quad (2)$$

$$\beta = \frac{H}{L\varepsilon} \quad (3)$$

$$A(\alpha_1) = -\frac{1}{\beta^2} - \alpha_1^2 \quad (4)$$

$$B(\alpha_1) = \alpha_1^4 \beta + \alpha_1^2 \left(\frac{2}{\beta} + 1 \right) + \frac{1}{\beta^3} + \frac{1}{\beta^2} \quad (5)$$

In the present study, the calculated value of β was larger than 67, so only the first three terms on the right side of Eq. (2) were adopted for calculating α_1^2 as the rest terms were negligible.

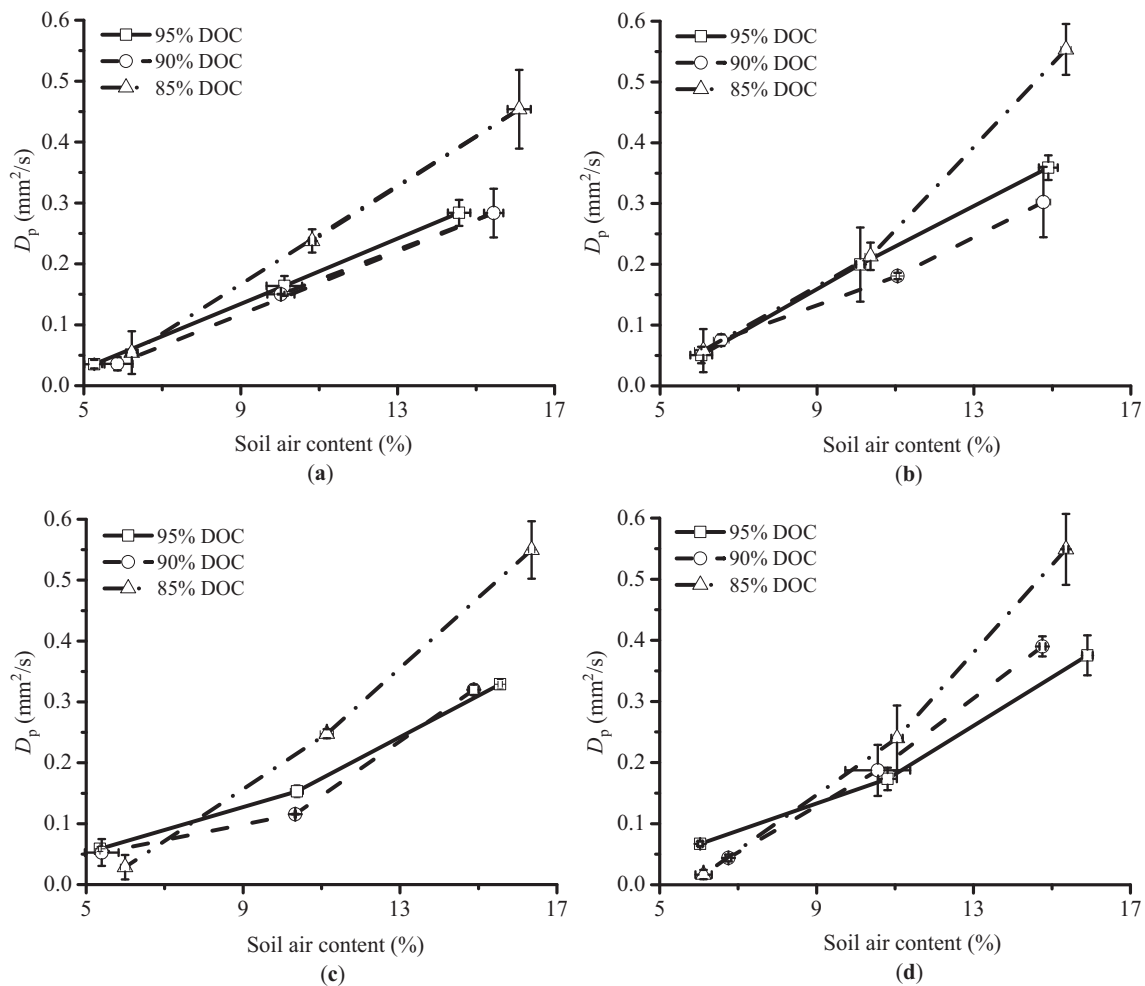


Fig. 4 Effects of soil air content (SAC) on gas diffusion coefficient (D_p) for soils amended with different biochar contents (BC) under different degree of compaction (DOC). **a** 0% BC. **b** 5% BC. **c** 10% BC. **d** 15% BC

The time plot of the measured oxygen concentrations was best fit using Eq. (1). Accordingly, the slope (i.e., $\eta = -\frac{D_p \alpha_1^2}{L^2 \varepsilon}$) of Eq. (1) could be determined. Thereafter, D_p was determined as follows:

$$D_p = -\frac{L^2 \varepsilon \eta}{\alpha_1^2} \quad (6)$$

Afterwards, the porosity, SAC, and degree of saturation (DS) were calculated according to the measured soil GWC and particle density. Three replicated tests were conducted to measure D_p of each soil sample amended with a given BC under a controlled DOC and SAC. In total, 108 soil samples were prepared and tested.

Micro-structure analysis by SEM

Two groups of test soil samples with the following target variables were selected for micro-structure analysis, i.e., (a) 10% BC, 10% SAC, and 85% DOC; and (b) 10% BC, 10% SAC, and 95% DOC. After measuring the D_p , a soil specimen with volume about 0.5 cm^3 was collected from the soil sample inside the cutting ring, dried at 45°C for 48 h, sprayed with a thin layer of gold, and then investigated by scanning electron microscopy (Nova Nano SEM 230; FEI Czech Republic s.r.o. Co., Ltd. in Czech; energy resolution 132 eV).

Statistical interpretation

One-way analysis of variance (ANOVA) and subsequent significant difference tests were conducted to analyze the measurements (Ng et al. 2018). The significance level of all ANOVA analyses was 0.05, corresponding to 95% confidence interval. Statistical analysis was performed using the statistical toolbox provided by Matlab (Matlab 2014). The standard deviation was calculated for all the data measured in repeated experiments, as shown in Table 2.

Results and discussion

Effects of biochar on soil compaction curve

Figure 2 shows the compaction curves of soils with different BCs. After the addition of biochar, the maximum dry density decreased, which was consistent with the reported findings in the literature (Garg et al. 2019; Reddy et al. 2014). It was due to that the particle density of the biochar is smaller than the soil used in the tests (Table 1). On the contrary, a larger optimum moisture content could be observed after adding biochar. It could be probably attributed to that the porosity of the biochar was larger than soil particles (Guo et al. 2014). Compared with the compaction curves of BAS to those of Garg et al.

(2019), a lower decrease in the maximum dry density and a larger increase in the optimum moisture content of the soil samples were observed in the present study (Fig. 2). It was likely because the biochar adopted in Garg et al. (2019) had a lower particle density (0.8 g/cm^3) than that in the present study (2.56 g/cm^3 , Table 1).

Effects of BC on D_p at different DOCs

Figure 3 shows a time series plot of oxygen concentration (C_g) for a set of repeat tests of soil samples with 0% BC, 10% SAC, and 85% DOC. Satisfactory fit with goodness of fit (R^2) larger than 95% could be obtained by using Eq. (1) through the least

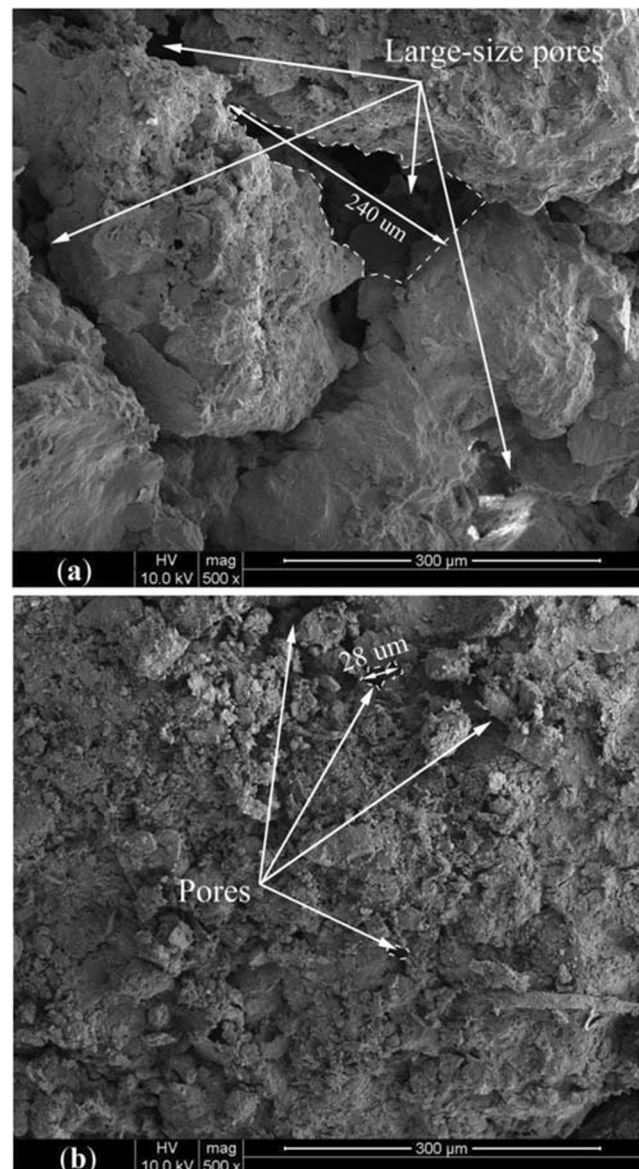
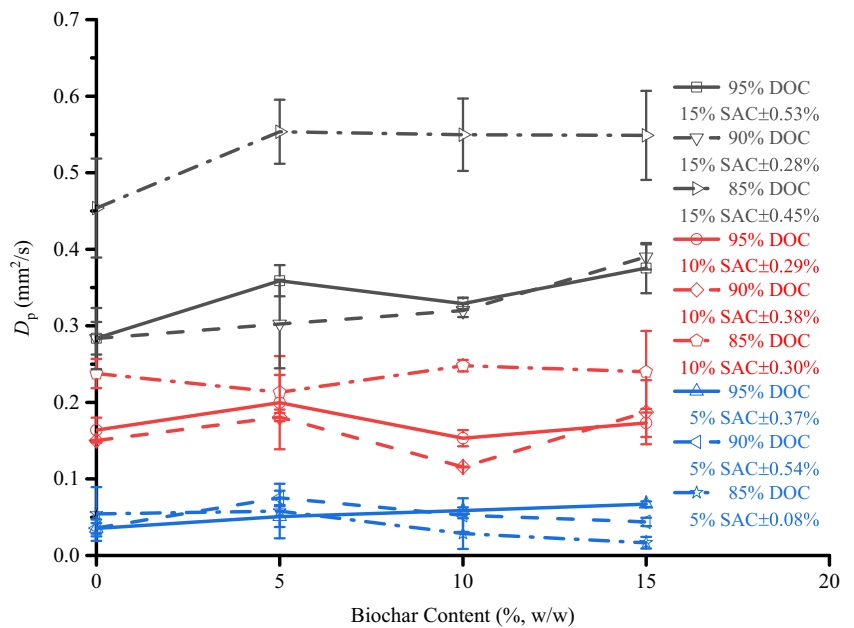


Fig. 5 Soil aggregates morphology at 500X magnification for soils with different BC, SAC, and DOC. **a** 10% BC, 10% SAC, 85% DOC. **b** 10% BC, 10% SAC, 95% DOC

Fig. 6 Effects of biochar content on D_p of soils with different DOC and SAC. SAC values are presented in mean \pm standard deviation



square method. Accordingly, D_p could be calculated using Eq. (6) and were summarized in Table. 2.

Figure 4 shows the relationship between D_p and SAC for soils amended with different BCs. In all test groups, D_p increased as SAC increased under a given DOC, which was consistent with the existing findings in the literature (Moldrup et al. 2000a; Hamamoto et al. 2011). It was because there were more gas-filled pores and the connectivity of these pores was improved under larger SAC. Under SAC of 5%, similar D_p could be observed for soil samples with different DOCs. It was likely due to the blockage of gas flow by water, as the DS corresponding to SAC of 5% was about 85% (Table 2), at/above which the gas phase generally became discontinuous (Qiu 2016). As SAC further increased to 15%, the D_p of soil samples with 85% DOC was significantly larger than those under larger DOC (90–95%), regardless of BC ($p < 0.05$). It was because that there were more relative amounts of large pores (pore diameter $d > 30 \mu\text{m}$) (Kuncoro et al. 2014) in soil samples with lower DOC, as shown in the two SEM images of soil samples with the same BC (10%), SAC (10%) but different DOCs of 95% and 85%, respectively (Fig. 5 a and b). It can be seen that the pore size of soil sample with low compactness (Fig. 5a) was larger than that with high compactness (Fig. 5b), since the large-size pores in soil would be preferentially compressed as DOC increased (Berisso et al. 2012; Kuncoro et al. 2014). Therefore, soil samples with 85% DOC might have more connected large-size pores at larger SAC, resulting in more available space, shorter flow paths, and reduced tortuosity of pores for gas diffusion and hence larger D_p (Allaire et al. 2008; Moldrup et al. 2000b).

Figure 6 shows the effects of BC on D_p of soils under different DOCs and SACs. When SAC was below 10%, BC had negligible effects on D_p ($p > 0.05$) under a given DOC and

SAC. It was likely due to that most of the pores in the BAS were filled by water, leading to a discontinuous gas phase. As the diffusion of gas in water is 3–4 orders of magnitude lower than that in the air, SAC dominated D_p under low SAC (Resurreccion et al. 2008b). As SAC further increased to 15%, the addition of biochar generally promoted the gas diffusion in soil, and the effect depended on DOC. For example, when the DOC was about 85%, the D_p increased as BC increased to 5% and remained substantially unchanged thereafter, while D_p generally increased with BC under larger DOC ($\geq 90\%$). This indicated that the relatively large-size pores in soils with DOC of 85% (Fig. 5a) dominated gas diffusion, while the addition of biochar might increase the pore connectivity under high DOC ($\geq 90\%$). A direct engineering implication of this finding is that biochar addition could be adopted to compromise the contradictory requirements of high DOC (e.g., $\geq 90\%$, leading to a reduced soil aeration) and high soil aeration (i.e., large D_p) in sloping landfill cover and man-made slope, where a high DOC is necessary for stability concern but a good aeration is needed for vegetation growth.

Conclusions

Effects of BC (0%, 5%, 10%, and 15%) on gas D_p of soil were measured by a two-chamber apparatus under different DOC (85%, 90%, and 95%) and SAC (5%, 10% and 15%). It was found that when SAC was less than about 5%, D_p was relatively low and controlled by SAC, regardless of DOC and BC. This was likely due to blockage of pore volume by water, resulting in less available space for gas flow and poor air-filled pore connectivity. On the contrary, when the SAC was

relatively high ($\geq 15\%$), soil with DOC of 85% had the largest D_p for DOC ranging from 85 to 95% under a given SAC. No noticeable difference could be observed for D_p under DOC of 90% and 95%. It was because soil samples with DOC of 85% had relatively larger pore size than those with higher DOC.

The influence of BC on D_p depended on SAC and DOC. When SAC was less than 10%, the influence of BC on D_p could be neglected. As SAC increased to about 15%, the D_p of soil samples with high DOC ($\geq 90\%$) generally increased with BC, while D_p increased with BC up to 5% and then remained basically unchanged under DOC of 85%. This indicated that gas diffusion was affected not only by available gas-filled pores but also by characteristics of pores (e.g., pore-size distribution, pore connectivity). Further effort is needed to investigate the effects of pore characteristic on D_p .

Author contributions All authors contributed to the study conception and design. Song Feng was in charge of this research. Neng Kai Zhao and Fu Quan Chen completed the test. Hong Wei Liu and Yu Chuan Liu conducted data analysis. Song Feng and Neng Kai Zhao drafted and revised the manuscript.

Funding information The authors would like to acknowledge (i) the National Natural Science Foundation of China for supporting research grants (51778166, 51808125, 51908134, 41861134011), and (ii) the Foundation of Key Laboratory of Soft Soils and Geoenvironmental Engineering (Zhejiang University), Ministry of Education, for supporting the project (2019P06); (iii) Natural Science Foundation of Fujian Province for supporting research grant (2017J01466).

References

- Adhikari S, Gasco G, Mendez A, Surapaneni A, Jegatheesan V, Shah K, Paz-Ferreiro J (2019) Influence of pyrolysis parameters on phosphorus fractions of biosolids derived biochar. *Sci Total Environ* 695: 133846. <https://doi.org/10.1016/j.scitotenv.2019.133846>
- Allaire SE, Lafond JA, Cabral AR, Lange SF (2008) Measurement of gas diffusion through soils: comparison of laboratory methods. *J Environ Monit* 10:1326–1336. <https://doi.org/10.1039/b809461f>
- ASTM D 2487 (2017) Standard practice for classification of soils for engineering purposes (unified soil classification system). American Society for Testing and Materials, West Conshohocken
- ASTM D 422 - 63 (2007) Standard test method for particle-size analysis. American Society for Testing and Materials, West Conshohocken
- ASTM D 4318 (2017) Standard test methods for liquid limit, plastic limit, and plasticity index of soils. American Society for Testing and Materials, West Conshohocken
- ASTM D 698 (2010) Standard test methods for laboratory compaction characteristics of soil using standard effort. American Society for Testing and Materials, West Conshohocken
- ASTM D 854 (2014) Standard test methods for specific gravity of soil solids by water pycnometer. American Society for Testing and Materials, West Conshohocken
- Berisso FE, Schjønning P, Keller T, Lamande M, Etana A, de Jonge LW, Iversen BV, Arvidsson J, Forkman J (2012) Persistent effects of subsoil compaction on pore size distribution and gas transport in a loamy soil. *Soil Tillage Res* 122:42–51. <https://doi.org/10.1016/j.still.2012.02.005>
- Bonroy J, Volckaert M, Seuntjens P (2011) Rapid automated measurement system for simultaneous determination of effective air-filled porosity and soil gas diffusivity. *Soil Sci Soc Am J* 75:408–417. <https://doi.org/10.2136/sssaj2010.0102>
- Boon A, Robinson JS, Nightingale PD, Cardenas L, Chadwick DR, Verhoef A (2013) Determination of the gas diffusion coefficient of a peat grassland soil. *Eur J Soil Sci* 64:681–687. <https://doi.org/10.1111/ejss.12056>
- Chen R, Ng CWW (2013) Impact of wetting–drying cycles on hydro-mechanical behavior of an unsaturated compacted clay. *Appl Clay Sci* 86:38–46. <https://doi.org/10.1016/j.clay.2013.09.018>
- Chen R, Liu J, Li JH, Ng CWW (2015) An integrated high-capacity tensiometer for measuring water retention curves continuously. *Soil Sci Soc Am J* 79:943–947. <https://doi.org/10.2136/sssaj2014.11.0438n>
- Chen XW, Wong JTF, Chen ZT, Tang TWL, Guo HW, Leung AOW, Ng CWW, Wong MH (2018) Effects of biochar on the ecological performance of a subtropical landfill. *Sci Total Environ* 644:963–975. <https://doi.org/10.1016/j.scitotenv.2018.06.379>
- Chen R, Ge Y, Chen Z, Liu J, Zhao Y, Li Z (2019a) Analytical solution for one-dimensional contaminant diffusion through unsaturated soils beneath geomembrane. *J Hydrol* 568:260–274. <https://doi.org/10.1016/j.jhydrol.2018.10.057>
- Chen R, Huang JW, Chen ZK, Xu Y, Liu J, Ge YH (2019b) Effect of root density of wheat and okra on hydraulic properties of an unsaturated compacted loam. *Eur J Soil Sci* 70:493–506. <https://doi.org/10.1111/ejss.12766>
- Chen R, Liu J, Ng CWW, Chen ZK (2019c) Influence of slope angle on water flow in a three-layer capillary barrier soil cover under heavy rainfall. *Soil Sci Soc Am J* 83:1637–1647. <https://doi.org/10.2136/sssaj2019.05.0135>
- Dane JH, Topp GC (2002) Methods of soil analysis. In: Moldrup P (ed) Rolston D.E. Gas Diffusivity, Madison, pp 1113–1139
- Fang Q, Chen B, Lin Y, Guan Y (2014) Aromatic and hydrophobic surfaces of wood-derived biochar enhance perchlorate adsorption via hydrogen bonding to oxygen-containing organic groups. *Environ Sci Technol* 48:279–288. <https://doi.org/10.1021/es403711y>
- Feng S, Liu HW, Chiu ACF, Ng CWW (2019) A steady-state analytical profile method for determining methane oxidation in landfill cover. *Sci Total Environ* 646:1528–1535. <https://doi.org/10.1016/j.scitotenv.2018.07.097>
- Garg A, Bordoloi S, Ni J, Cai W, Maddibiona PG, Mei G, Poulsen TG, Lin P (2019) Influence of biochar addition on gas permeability in unsaturated soil. *Geotechnique Letters* 9:66–71. <https://doi.org/10.1680/jgele.18.00190>
- Glauz RD, Rolston DE (1989) Optimal design of two-chamber, gas diffusion cells. *Soil Sci Soc Am J* 53:1619–1624. <https://doi.org/10.2136/sssaj1989.03615995005300060001x>
- Gopal P, Bordoloi S, Ratnam R, Lin P, Cai W, Buragohain P, Garg A, Sreedeeep S (2019) Investigation of infiltration rate for soil-biochar composites of water hyacinth. *Acta Geophysica* 67:231–246. <https://doi.org/10.1007/s11600-018-0237-8>
- Guo Y, Tang H, Li G, Xie D (2014) Effects of cow dung biochar amendment on adsorption and leaching of nutrient from an acid yellow soil irrigated with biogas slurry. *Water Air Soil Pollut* 225. <https://doi.org/10.1007/s11270-013-1820-x>
- Hamamoto S, Moldrup P, Kawamoto K, Wickramarachchi PN, Nagamori M, Komatsu T (2011) Extreme compaction effects on gas transport parameters and estimated climate gas exchange for a landfill final cover soil. *J Geotech Geoenviron* 137:653–662. [https://doi.org/10.1061/\(ASCE\)GT.1943-5606](https://doi.org/10.1061/(ASCE)GT.1943-5606)
- Iberahim N, Sethupathi S, Bashir MJK (2018) Optimization of palm oil mill sludge biochar preparation for sulfur dioxide removal. *Environ Sci Pollut Res* 25:25702–25714. <https://doi.org/10.1007/s11356-017-9180-5>

- Kuncoro PH, Koga K, Satta N, Muto Y (2014) A study on the effect of compaction on transport properties of soil gas and water. II: Soil pore structure indices. *Soil Tillage Res* 143:180–187. <https://doi.org/10.1016/j.still.2014.01.008>
- Lei O, Zhang R (2013) Effects of biochars derived from different feedstocks and pyrolysis temperatures on soil physical and hydraulic properties. *J Soils Sediments* 13:1561–1572. <https://doi.org/10.1007/s11368-013-0738-7>
- Lipiec J, Hom R, Pietrusiewicz J, Siczek A (2012) Effects of soil compaction on root elongation and anatomy of different cereal plant species. *Soil Tillage Res* 121:74–81. <https://doi.org/10.1016/j.still.2012.01.013>
- Liu C, Wang H, Tang X, Guan Z, Reid BJ, Rajapaksha AU, Ok YS, Sun H (2016) Biochar increased water holding capacity but accelerated organic carbon leaching from a sloping farmland soil in China. *Environ Sci Pollut Res* 23:995–1006. <https://doi.org/10.1007/s11356-015-4885-9>
- MATLAB 2014 Reference manual. MATLAB, Inc., MathWorks, America
- Millington RJ, Quirk JP (1961) Permeability of porous solids. *Trans Faraday Soc* 57:1200–1207. <https://doi.org/10.1039/TF9615701200>
- Moldrup P, Olesen T, Gamst J, Schjøning P, Yamaguchi T, Rolston DE (2000a) Predicting the gas diffusion coefficient in repacked soil: water-induced linear reduction model. *Soil Sci Soc Am J* 64:1588–1594. <https://doi.org/10.2136/sssaj2000.6451588x>
- Moldrup P, Olesen T, Schjøning P, Yamaguchi T, Rolston DE (2000b) Predicting the gas diffusion coefficient in undisturbed soil from soil water characteristics. *Soil Sci Soc Am J* 64:94–100. <https://doi.org/10.2136/sssaj2000.64194x>
- Ng CWW, So PS, Coo JL, Zhou C, Lau SY (2018) Effects of biofilm on gas permeability of unsaturated sand. *Géotechnique*. 1-7. <https://doi.org/10.1680/jgeot.17.T.042>
- Qiu QW (2016) Study on moisture-gas coupled flow in loess/gravel final cover and control of landfill gas emission. Ph.D thesis, Zhejiang University, China (in Chinese)
- Reddy KR, Yargicoglu EN, Yue D, Yaghoubi P (2014) Enhanced microbial methane oxidation in landfill cover soil amended with biochar. *J Geotech Geoenviron* 140:04014047. [https://doi.org/10.1061/\(asce\)gt.1943-5606.0001148](https://doi.org/10.1061/(asce)gt.1943-5606.0001148)
- Resurreccion AC, Komatsu T, Kawamoto K, Oda M, Yoshikawa S, Moldrup P (2008a) Linear model to predict soil-gas diffusivity from two soil-water retention points in unsaturated volcanic ash soils. *Soils Found* 48:397–406. <https://doi.org/10.3208/sandf.48.397>
- Resurreccion AC, Moldrup P, Kawamoto K, Yoshikawa S, Rolston DE, Komatsu T (2008b) Variable pore connectivity factor model for gas diffusivity in unsaturated, aggregated soil. *Vadose Zone J* 7:397–405. <https://doi.org/10.2136/vzj2007.0058>
- Sanford JR, Larson RA, Runge T (2019) Nitrate sorption to biochar following chemical oxidation. *Sci Total Environ* 669:938–947. <https://doi.org/10.1016/j.scitotenv.2019.03.061>
- Schjøning P (1989) Long-term reduced cultivation. II soil pore characteristics as shown by gas diffusivities and permeabilities and air-filled porosities. *Soil Tillage Res* 15:91–103. [https://doi.org/10.1016/0167-1987\(89\)90066-4](https://doi.org/10.1016/0167-1987(89)90066-4)
- Schjøning P, Eden M, Moldrup P, de Jonge LW (2013) Two-chamber, two-gas and one-chamber, one-gas methods for measuring the soil-gas diffusion coefficient: validation and inter-calibration. *Soil Sci Soc Am J* 77:729–740. <https://doi.org/10.2136/sssaj2012.0379>
- Senbayram M, Saygan EP, Chen RR, Aydemir S, Kaya C, Wu D, Bladogatskaya E (2019) Effect of biochar origin and soil type on the greenhouse gas emission and the bacterial community structure in N fertilised acidic sandy and alkaline clay soil. *Sci Total Environ* 660:69–79. <https://doi.org/10.1016/j.scitotenv.2018.12.300>
- Shang G, Shen G, Liu L, Chen Q, Xu Z (2013) Kinetics and mechanisms of hydrogen sulfide adsorption by biochars. *Bioresour Technol* 133:495–499. <https://doi.org/10.1016/j.biortech.2013.01.114>
- Su CC, Ma JF, Chen YP (2019) Biochar can improve the soil quality of new creation farmland on the Loess Plateau. *Environ Sci Pollut Res* 26:2662–2670. <https://doi.org/10.1007/s11356-018-3550-5>
- Sun HJ, Lu HY, Feng YF (2019) Greenhouse gas emissions vary in response to different biochar amendments: an assessment based on two consecutive rice growth cycles. *Environ Sci Pollut Res* 26:749–758. <https://doi.org/10.1007/s11356-018-3636-0>
- Tan G, Wang H, Xu N, Liu H, Zhai L (2018) Biochar amendment with fertilizers increases peanut N uptake, alleviates soil N₂O emissions without affecting NH₃ volatilization in field experiments. *Environ Sci Pollut Res* 25:8817–8826. <https://doi.org/10.1007/s11356-017-1116-6>
- Wall A, Heiskanen J (2009) Soil–water content and air-filled porosity affect height growth of Scots pine in afforested arable land in Finland. *For Ecol Manag* 257:1751–1756. <https://doi.org/10.1016/j.foreco.2009.01.029>
- Wong JTF, Chen ZK, Ng CWW, Wong MH (2016) Gas permeability of biochar-amended clay: potential alternative landfill final cover material. *Environ Sci Pollut Res* 23:7126–7131. <https://doi.org/10.1007/s11356-015-4871-2>
- Wong JTF, Chen ZK, Chen XW, Ng CWW, Wong MH (2017) Soil-water retention behavior of compacted biochar-amended clay: a novel landfill final cover material. *J Soils Sediments* 17:590–598. <https://doi.org/10.1007/s11368-016-1401-x>
- Wu S, He H, Inthapanya X, Yang C, Lu L, Zeng G, Han Z (2017) Role of biochar on composting of organic wastes and remediation of contaminated soils—a review. *Environ Sci Pollut Res* 24:16560–16577. <https://doi.org/10.1007/s11356-017-9168-1>
- Xu X, Cao X, Zhao L, Sun T (2014) Comparison of sewage sludge- and pig manure-derived biochars for hydrogen sulfide removal. *Chemosphere*. 111:296–303. <https://doi.org/10.1016/j.chemosphere.2014.04.014>
- Yargicoglu EN, Reddy KR (2017) Effects of biochar and wood pellets amendments added to landfill cover soil on microbial methane oxidation: a laboratory column study. *J Environ Manag* 193:19–31. <https://doi.org/10.1016/j.jenvman.2017.01.068>
- Zhang C, Liu L, Zhao M, Rong H, Xu Y (2018) The environmental characteristics and applications of biochar. *Environ Sci Pollut Res* 25:21525–21534. <https://doi.org/10.1007/s11356-018-2521-1>

Publisher's note Springer Nature remains neutral with regard to jurisdictional claims in published maps and institutional affiliations.